



Prediction models for shape and size of ca-alginate macrobeads produced through extrusion–dripping method

Eng-Seng Chan^{a,*}, Boon-Beng Lee^a, Pogaku Ravindra^a, Denis Poncelet^b

^a Centre of Materials and Minerals, School of Engineering and Information Technology, Universiti Malaysia Sabah, 88999 Kota Kinabalu, Sabah, Malaysia

^b ENITIAA: rue de la Géraudière, B.P. 82225, 44332 NANTES Cedex 3, France

ARTICLE INFO

Article history:

Received 7 February 2009

Accepted 11 May 2009

Available online 19 May 2009

Keywords:

Shape

Size

Extrusion

Bead

Drop

Encapsulation

Alginate

ABSTRACT

The aim of this work was to develop prediction models for shape and size of ca-alginate macrobeads produced through extrusion–dripping method. The relationship between the process variables on the shape and size of the alginate drops before and after gelation was established with the aid of image analysis. The results show that a critical Ohnesorge number (Oh) > 0.24 was required to form spherical beads. The shape transition of ca-alginate beads could be typically distinguished into three phases along the collecting distance and it was affected by the combined influence of the solution properties, the collecting distance and the drop size. Mathematical equations and a master shape diagram were developed to reveal a clear operating region and the overall process limits within which spherical ca-alginate beads could be formed. In terms of bead size, the overall size correction factor (K) which accounted for the liquid loss factor (k_{LF}) and the shrinkage factor (k_{SF}), varied between 0.73 and 0.85 under the experimental conditions. The size prediction model correlated well with the experimental data. The approach and the outcome could be used as a model to develop prediction tools for similar bead production systems.

© 2009 Elsevier Inc. All rights reserved.

1. Introduction

Encapsulation could be defined as a process of confining active compounds within a matrix in particulate form to achieve one or more desirable effects. To date, there are numerous articles that report on the successful use of carrier particles, in wet or dry form (in a process or as part of product). The particles could be used to achieve one or a combination of the encapsulation objectives such as immobilization, protection (or stabilization), controlled-release and alteration of product properties [1–6].

Alginate is one of the most widely used materials for encapsulation. It is a natural polysaccharide derived from marine plant and its basic structure consists of linear unbranched polymers containing β -(1 \rightarrow 4)-linked D-mannuronic acid (M) and α -(1 \rightarrow 4)-linked L-guluronic acid (G) residues. It can form thermally stable and biocompatible hydrogel in the presence of calcium cation. In addition, the hydrogel can be easily produced into particulate form by using simple and gentle method. It has been used in many encapsulation applications such as in the field of biomedical, bio-process, pharmaceutical, food and feed. Examples of the encapsulated compounds are such as microbial cells, enzymes, hormones, drugs, oils and flavours [2–4,7–9].

The critical design considerations of alginate particles are highly dependent on the applications. Among the considerations are the

size, size distribution, shape, mass transport properties, biocompatibility, swelling properties, solubility, mechanical and chemical stability. The carrier qualities could be influenced by the alginate composition and concentration, the presence of impurities, the type and concentration of gelling ions and non-gelling ions as well as the production process conditions. In the recent years, it has become a common trend to produce mono-dispersed as well as perfectly spherical ca-alginate particles. The reasons could be:

- (i) To develop highly reproducible reaction or controlled-release rates which may be critical in some biomedical, pharmaceutical and bioprocess applications.
- (ii) To develop free-flowing particles during dosing and handling in order to ensure dosage consistency and dust-free environment (due to particle abrasion) which could be the requirement for pharmaceutical, food and feed applications.
- (iii) To improve the aesthetic quality which could be a desirable characteristic for pharmaceutical, food and feed products.

The most classic and popular way to produce mono-dispersed and round ca-alginate macrobeads is by using the dripping technique. In this method, the alginate solution is extruded through a capillary at a low volumetric rate and allowed to drip under gravity. Although this method has been used for many years, formation of the beads with desired size and spherical-shaped often requires some trial and error works on the liquid formulation and experimental set-up (e.g. solution viscosity or surface tension, tip size,

* Corresponding author. Fax: +60 88 320 348.

E-mail addresses: chan@ums.edu.my, engseng.chan@gmail.com (E.-S. Chan).

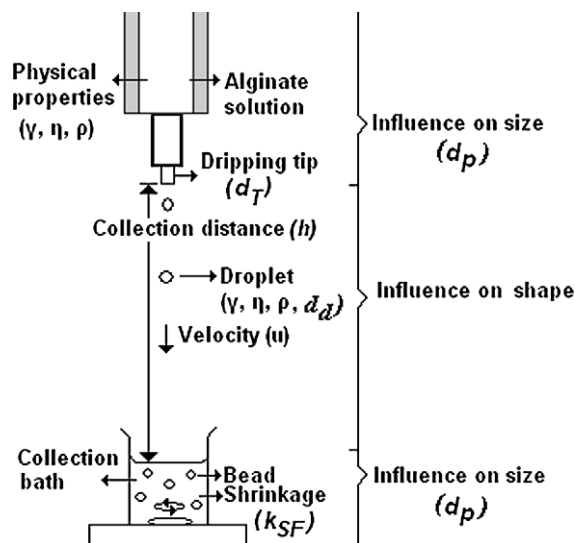


Fig. 1. Schematic of the process variables involved in formation of ca-alginate beads.

collecting distance etc.). If the conditions are not optimum, deformed beads or beads with tail could be produced, as shown in some of the previous works [2,9–12]. On the other hand, the size of the beads produced is commonly predicted by the Tate's law [13–15], which approximates the balance between the gravitational force pulling the drop down and the surface tension force holding the drop pendant to the tip at the instant of drop detachment. In reality, the actual size of the ca-alginate beads was found to be smaller than predicted.

Until now, there are limited efforts to develop models that comprehensively correlate the material properties and experimental conditions on the shape and size of the beads formed. The aim of this work is to develop prediction models for shape and size of the ca-alginate macrobeads produced by the extrusion–dripping method. An empirical approach was used by determining the relationship between the process variables (i.e. material properties and experimental set-up) on the shape and the size of alginate drop before and after gelation, as shown in Fig. 1. A dimensionless shape indicator and visual images were used for shape analysis and the shape diagrams were developed. On the other hand, the size prediction model was developed by modifying the Tate's law with the overall size correction factor (K). The correction factor was established by dividing the drop size analysis into two parts. Firstly, the partial detachment of alginate liquid pendant from the dripping tip was quantified and it is known as the liquid lost factor (k_{LF}). Secondly, the shrinkage of alginate drops was determined and it is known as the shrinkage factor (k_{SF}). The applicability and limitations of the size prediction model was then discussed.

2. Materials and methods

2.1. Materials

Two commercially available alginates (Manugel GHB and Manucol DH) were used in this study and they were kindly donated by ISP Alginates (United Kingdom). Medium molecular weight alginates were used because they are commonly used for encapsulation applications. In this study, the alginates with different M/G ratio, but nearly same molecular weight, were chosen. Their properties are summarized in Table 1. The information was provided by the manufacturer and they were based on estimation due to batch-to-batch variability.

Table 1
Typical properties of alginate used in this study.^a

Alginate type	Manugel GHB	Manucol DH
Molecular weight	~97,000	~97,000
M:G ratio ^b	~0.59	~1.56
Viscosity at 10 g/L (mPa s) ^c	50–100	40–90
Loss on drying (%) ^d	<13	<13
Ash (dried basis) (%) ^e	18–27	18–27
Heavy metals (ppm)	<1.9	<1.3

^a Information was provided by the manufacturer and they were based on estimation due to batch-to-batch variability.

^b The ratio of uronic acid content of alginate [β -D-mannuronic acid residues (M) and α -L-guluronic acid residues (G)].

^c Viscosity was generally measured by using a Brookfield LV viscometer at 60 rpm with spindle no. 2.

^d Sample (5–10 g) was dried in a oven at 105 °C for 4 h and reweighed.

^e Determined according to the procedure given in Food Chemicals Codex.

2.2. Measurement of solution properties

The density of alginate solutions was measured by using a digital specific gravity meter (Kyoto Electronics Manufacturing Co. Ltd., Japan). The viscosity of the solutions was determined by using a viscometer according to the standard procedure (Brookfield Engineering Laboratories, Inc., Model: LV-DV E203, USA). The surface tension of the alginate solutions was determined by method as described in Lee et al. [16].

In this paper, the liquid properties of alginate drop are described by using the Ohnesorge number (Oh) which measures the importance of the viscous force to surface tension force of the liquid drop. The Ohnesorge number (Oh) is expressed by the following equation:

$$Oh = \nu / (\rho d_d \gamma)^{1/2} \quad (1)$$

where ν is the kinematic viscosity of the alginate solution (mm^2/s), ρ is the density of the alginate solution (kg/m^3), d_d is diameter of alginate liquid drop (mm), γ is the surface tension of the alginate solution (mN/m).

2.3. Experimental set-up

The experimental set-up for studying the shape and size of alginate liquid drops and ca-alginate beads is shown in Fig. 1. All studies were conducted at controlled temperature of 25 °C. Hypodermic needles (Precision needle, Singapore) of outer diameter from 0.40 to 1.65 mm were used as dripping tips. The length of the needles was shortened to 3 mm and the tip was flattened. The flow rate of alginate solution was adjusted to give an elapse time of 30 s between each drop so that the kinetic force generated during drop accumulation can be neglected. The gelling bath was prepared from calcium chloride (10 mM) and Tween 80 (1 g/L). The liquid properties of the gelling bath were not varied in this experiment. The collecting distance between the dripping tip and gelation bath was varied from 1 to 270 cm. The hardening time of the ca-alginate beads was fixed at 30 min. A digital camera (Canon, Japan) was set up below the dripping tip to capture the images of falling alginate liquid drops.

2.4. Shape analysis

The images of the alginate drops during falling (before gelation) and after gelation were captured for shape analysis. The shape of the alginate drops were quantified by using the dimensionless shape indicators as described in Table 2. The measurement was performed by using an image analyser (SigmaScan Pro 5, USA) and computed by using Microsoft Excel. The influence of the process parameters on the sphericity of the beads was established.

2.5. Size analysis

The size analysis of the alginate drops before and after gelation was mainly performed by using image analysis. The size prediction model for ca-alginate beads was developed by taking into account the liquid lost factor (k_{LF}) and the shrinkage factor (k_{SF}). The product of these factors could be expressed as the overall size correction factor (K). It could be used to modify the Tate's law, as described by Eq. (2):

$$d_p = k_{LF}k_{SF}(0.006d_T\gamma/\rho g)^{1/3} = K(0.006d_T\gamma/\rho g)^{1/3} \quad (2)$$

where d_p is the diameter of ca-alginate bead (mm), d_T is the outer diameter of tip (mm), ρ is the density of alginate solution (kg/m^3), g is the gravitational force ($9.81 \text{ m}/\text{s}^2$), γ is the surface tension of alginate solution (mN/m).

The liquid lost factor (k_{LF}) could be determined by first finding out the fraction of the ideal drop volume, $V_{\text{real}}/V_{\text{ideal}}$. Ideal drop volume (V_{ideal}) is defined as the theoretical volume of a liquid drop that detaches from a capillary and it can be predicted by using Tate's law [17]. The fraction could be obtained from an experimental master curve developed by Harkins and Brown (HB) [18]. The curve is a plot of the fraction of the ideal drop volume as a function of the dimensionless tip radius, $r/V_{\text{real}}^{1/3}$ where r is the tip radius. Once the $r/V_{\text{real}}^{1/3}$ is determined, the fraction of ideal drop volume can be obtained from the curve. The liquid lost factor (k_{LF}) could then be determined from Eq. (3):

$$k_{LF} = [V_{\text{real}}/V_{\text{ideal}}]^{1/3} \quad (3)$$

On the other hand, the mean shrinkage ratio was referred as the shrinkage factor (k_{SF}). It could be determined by comparing the diameter of the alginate drops before gelation and after gelation. The diameter of the alginate drops were measured by using the image analyzer. The shrinkage factor (k_{SF}) could be described as follows:

$$k_{SF} = d_p/d_d \quad (4)$$

where d_d and d_p are the diameters (mm) of alginate drop before gelation and after gelation respectively.

The overall size correction factor (K) was then calculated and the modified Tate's law (Eq. (2)) was then verified with experimental data to determine the accuracy and applicability in predicting the size of ca-alginate beads.

3. Results and discussion

3.1. Physical properties of alginate solution

The physical properties of alginate solutions at various concentrations are shown in Table 3. As the alginate concentration increased, the solution density increased slightly whereas the solution apparent viscosity at zero shear rate exhibited a typical

exponential increment. This is in good agreement with the previous studies [12,19,20]. It has also been reported that the rheological property of alginate solution is dependent on the shear rate [3,21–23]. Therefore, the rheology of the alginate solutions used in this study were examined with shear rates up to 30/s since it was found that the typical shear rates for extrusion process under gravity were between 0.1/s to 10/s [24]. Within this range of shear rates, the rheograms clearly show that the alginate solutions behaved like Newtonian fluids, regardless of the alginate concentration and M/G ratio (data not shown).

The surface tension at low alginate concentration (5–20 g/L) was about 68–72 mN/m and it showed a decreasing trend as the concentration increased. The results are in good agreement with previous findings [10,20,25] where the surface tension of solutions at low alginate concentration was found to be close to the surface tension of water (about 72 mN/m). This could be explained by the fact that the alginate is a hydrophilic polysaccharide hydrocolloid and it has low surface tension activity. On the other hand, some studies reported significantly lower surface tension (about 50–65 mN/m) at low alginate concentration [19,26]. The discrepancy could be attributed to many reasons such as the source of alginates, the presence of impurities and the method used to measure surface tension of the solutions.

In this work, the properties of alginate liquid drop are described by using the Ohnesorge number (Oh). The purpose is to take into account the effect of surface tension force in determining the drop size and drop shape during drop detachment, during falling or impaction [27,28], although its influence could have been subdued by the solution viscosity. Within the experimental limits of this study, the Oh is in the range of 0.075–13 (see Table 3).

3.2. Shape analysis of alginate drops

For shape analysis, the varied parameters were the alginate concentrations (5–50 g/L), tip diameter (0.4–1.6 mm) and the collecting distance (1–270 cm). The highest Ohnesorge number is given by 11–13 (alginate concentration of 50 g/L) since the solution was very viscous and it was difficult to process by using our apparatus. The liquid was dropped into a quiescent gelling bath containing calcium chloride (10 mM) and Tween 80 (1 g/L). The surface tension and the viscosity of the gelling solution were about 54 mN/m and 1 mPa s, respectively. The gelling bath condition was not altered since it is normally used in extrusion method.

Table 4 depicts the typical shapes of the alginate drops, from spherical to the elongated shape and the results obtained by using different dimensionless shape indicators. The circularity was found to be less sensitive to the elongation of the alginate drop. The aspect ratio gave good description of large deformations but small distortion was suppressed. On the other hand, the sphericity factor could describe the relative change of the drop shape more efficiently and thus, it was adopted in this study. A drop was considered spherical if the sphericity factor <0.05. This is because the

Table 2
Description of dimensionless shape indicators.

Shape indicator	Equation	Remarks
Circularity (C)	$C = P^2/4\pi A$	The circularity varies from unity for a perfect sphere to infinity for a non-spherical object
Aspect ratio (AR)	$AR = d_{\text{max}}/d_{\text{min}}$	The AR varies from unity for a perfect sphere to approaching infinity for an elongated particle
Sphericity factor (SF)	$SF = (d_{\text{max}} - d_{\text{min}})/(d_{\text{max}} + d_{\text{min}})$	The deformation factor varies from 0 for a perfect sphere to approaching unity for an elongated object

Note: P , perimeter (mm); A , area (mm^2); d_{max} , maximum diameter (mm); d_{min} , minimum diameter perpendicular to d_{max} (mm).

Table 3
Physical properties of alginate solutions.

Alginate concentration ^a (g/L)	Density ^b (kg/m^3)	Viscosity ^b (mPa s)	Surface tension ^b (mN/m)	Oh^c
5	999	38	71	0.075–0.093
15	1004	130	70	0.24–0.3
25	1008	560	69	1.1–1.3
40	1017	2700	57	5.8–6.5
50	1023	4700	47	11–13

^a Based on Manugel GHB.

^b Measurements were done in replicate and coefficient of variance is less than 5%.

^c Calculated based on Eq. (1) with tip diameter (d_T) ranging from 0.40 to 1.65 mm.

Table 4
Comparison of dimensionless shape indicators.

Dimensionless shape indicator				
Circularity	1.1	1.1	1.2	1.4
Aspect ratio	1.0	1.1	1.2	1.6
Sphericity factor	0.0016	0.050	0.077	0.22

extent of deformation could not be obviously differentiated by human vision.

It was found that the minimum alginate concentration required to enable the formation of spherical bead was 15 g/L. The critical Ohnesorge number (Oh) was found to be 0.24 (see Table 3). Previ-

ous works have shown that the viscosity of alginate solution must be above a certain range (i.e. 60–50 mPa s), to form spherical beads [2,10–12,29]. When an alginate liquid drop hits and enters the gelling bath, there are competing forces between the viscous–surface tension forces and impact-drag forces to maintain the drop shape. For solution with $Oh < 0.24$ (i.e. alginate concentration 0.5 g/L), the viscous and surface tension forces were lower than the minimum forces required to counter-act the effect of impact and drag. Therefore, spherical beads could not be formed regardless of the collecting distance.

Fig. 2a and b show the shape transition of alginate liquid drops and the ca-alginate formed at varying falling or collecting distance, as quantitatively indicated by the change in the sphericity factor. Also, the shape of liquid drop or bead could be classified into four basic types: spherical-shaped, tear-shaped, pear-shaped and egg-shaped (see Fig. 3). Tear-shaped describes a drop which is round

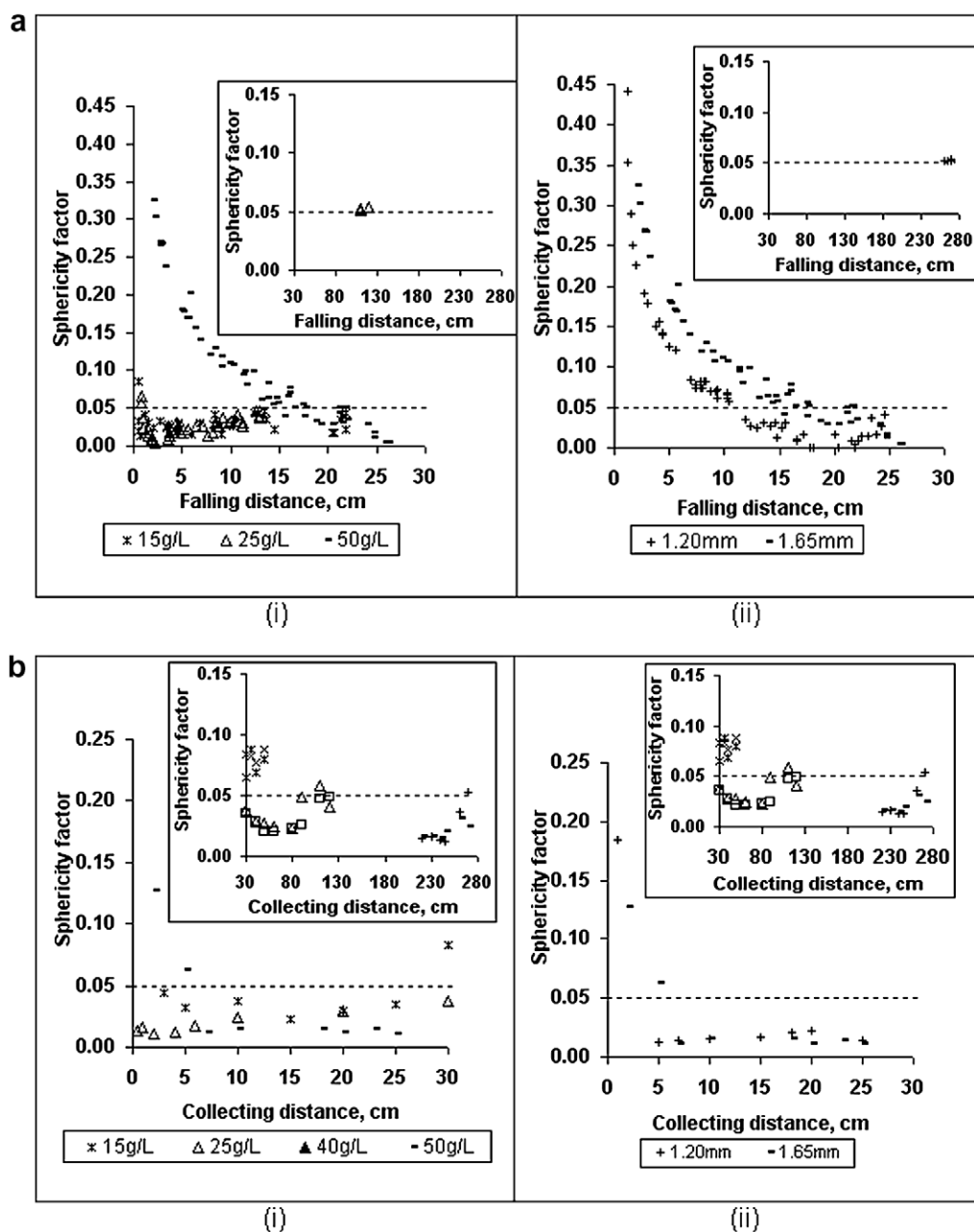


Fig. 2. (a) Shape transition of liquid drop at varying distance: (i) effect of alginate concentration (dripping tip: 1.65 mm), (ii) effect of tip size (50 g/L). (b) Shape transition of ca-alginate beads at varying distance: (i) effect of alginate concentration (dripping tip: 1.65 mm), (ii) effect of tip size (50 g/L).

at the bottom and narrowing towards the top, such as a drop with a distinct tail. A pear-shaped drop has similar characteristics but without a distinct tail and it resembles a pear. The egg-shaped drop resembles a chicken egg or an ellipsoidal.

One problem encountered was that the image analysis might not be able to detect a bead with very short tail as the sphericity factor of these particles could be < 0.05 . Under the experimental conditions, this type of particle was normally formed from alginate concentration between 15 and 40 g/L at very short collecting distance (i.e. < 3 cm). However, the difference could be distinguished by the shape transition pattern at the beginning of the collecting distance, as highlighted in Fig. 2b. In these cases, the sphericity factor was found to decrease sharply before reaching a threshold value. In addition to this, images of the particles were also used in parallel for comparison and verification in the shape analysis.

In general, for alginate solution with $Oh > 0.24$, the shape transition of the Ca-alginate beads with increasing collecting distance could be distinguished into three phases that follows the trend of tear-shaped (phase I) \rightarrow spherical (phase II) \rightarrow egg-shaped (phase III), as shown in Fig. 3. On the other hand, for $Oh < 0.24$, the bead was tear- or pear-shaped at short collecting distance and pear-shaped at long collecting distance. The shape transition of liquid drop in these phases is also shown in parallel for the ease of comparison. This enables systematic discussion on the drop shape that could be caused by different mechanisms.

The first phase involves the range of collecting distance right after detachment of liquid drops from the dripping tip. In this phase, the liquid drop shape could have significant influence on the bead shape. When a liquid drop detached from a capillary, it appeared in tear-shaped. Due to the surface tension effect, the shape of a falling drop evolved from tear-drop shaped to egg-shaped before it eventually became spherical, as also indicated by the decreasing sphericity factor in Fig. 2. If a tear-shaped liquid drop was collected, the liquid drop shape could be partially preserved during impact. This could result in a bead with a distinct tail. This effect was magnified when the liquid drop was produced

from the highest alginate concentration (i.e. 50 g/L) and the largest tip (i.e. 1.65 mm)(see Fig. 2a and b).

The second phase involves the range of collecting distance that forms spherical Ca-alginate beads with sphericity factor < 0.05 . Within this distance, the viscous and the surface tension forces of a liquid drop could overcome the impact force and drag force exerted when the drop hits and enters the gelling bath. However, the sphericity factor was generally found to increase steadily albeit slowly as the collecting distance was increased further. This was an indication of shape deformation due to increasing degree of impact-drag force although the shape distortion was not clearly visible for human eyes.

On the other hand, it was found that the spherical bead could also be formed from a liquid drop that is less spherical before impaction (i.e. sphericity factor > 0.05). This effect could be seen in the liquid drop produced from most alginate concentrations, especially the 50 g/L concentration. Spherical beads were formed at a collecting distance of about 7 cm when the falling liquid drops at the corresponding distance were obviously non-spherical (i.e. sphericity factor = 0.08–0.14). In contrast to the common belief that impact causes drop deformation, this range of collecting distance could help to rearrange the shape of the liquid drop upon impact to form spherical beads. This is provided that the liquid drop is near spherical, such as an egg-shaped drop.

When the liquid drop falls beyond the second phase of the collecting distance, deformed beads with an egg shape were normally produced. This could be possibly explained by two different mechanisms. As a liquid drop falls at long distance, there are increasing competing forces between the surface tension–viscosity of the drop and the pressure of the air pushing up against the bottom of the drop. This effect could be seen from the sphericity factors of liquid drop, where they increased steadily, but not obviously, with longer falling distance. However, our results show that the liquid drop remained generally spherical before impaction. Therefore, the shape deformation should be mainly caused by impaction where the viscous and the surface tension forces of

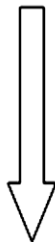
Falling or collecting distance	Phase	Alginate liquid drop		Ca-alginate beads			
				< critical Oh		> critical Oh	
	I	Tear		Tear/Pear		Tear	
		↓	Egg		↓		↓
	II	Egg		Pear		Spherical	
		↓	Spherical				
	III	Spherical		Pear		Egg	

Fig. 3. Shape transition of alginate drops.

the liquid drop could not overcome the impact force exerted when it hit the gelling bath.

Based on the experimental data, a diagram that relates the collecting distance and liquid properties to form spherical beads could be proposed (see Fig. 4). Within the limits of the liquid properties, spherical beads could be formed if an alginate liquid drop was collected between the minimum collecting distance and the maximum collecting distance. The first distance was to avoid formation of tear-shaped beads and the second distance was to avoid shape deformation. Within the experimental conditions, the minimum and maximum collecting distances were found to be correlated with the Ohnesorge number. Regression analysis shows a strong correlation between the distances and the liquid properties for both equations with a coefficient of determination, $R^2 = 0.98$. On the other hand, the drop size was found to have relatively less significant influence over the liquid properties under the experimental conditions. The equations are as shown in Eqs. (5) and (6):

$$D_{\min} = 1.63e^{0.12 Oh} \tag{5}$$

$$D_{\max} = 62.35 \ln(Oh) + 111 \tag{6}$$

where D_{\min} (cm) is the minimum collecting distance and D_{\max} (cm) is the maximum collecting distance.

The minimum and maximum collecting distances are strongly dependent on the viscosity of the solution. Since the solution viscosity increased exponentially with the alginate concentration, this explains the exponential and natural-logarithmic relationship between the collecting distances and Oh . The diagram also estab-

lished the basis for the common practice of setting the collecting distance at 10 cm when this method is used to produce alginate beads. At this distance, spherical beads can be produced from a wide range of solution properties. However, the minimum collecting distance can be varied if required where the lowest possible distance is about 2 cm (as Eq. (5) converges on 1.63 cm).

With the aid of the collecting distance vs. Oh diagram, the process requirements with respect to the liquid formulation, drop size and collecting distance could be easily optimized or manipulated to form spherical beads. However, the main limitation of the diagram is that it can only be used for the extrusion–dripping system. It will be desirable if the application of shape diagram could be extended to other extrusion systems (e.g. jet-cutter, vibration break-up of liquid jet, electrostatic generator) that may also involve impaction between the liquid drop and gelling bath to form calginate beads. In view of this, further analysis was performed from the perspective of liquid–liquid impact by using the extrusion–dripping system as a model.

From our study, it was found that the degree of impact between the liquid drop and gelling bath could have desirable or non-desirable effect on the bead shape depending on which transition phase was involved. The degree of impact depends on the momentum of a liquid drop, which can be manipulated with the collecting distance. In brief, momentum could be defined as the product of the mass and velocity of an object. A larger liquid drop or a longer collecting distance (i.e. higher velocity) increases the momentum of a falling drop. As a result, the degree of impact between the drop and the surface of the gelling bath would be greater.

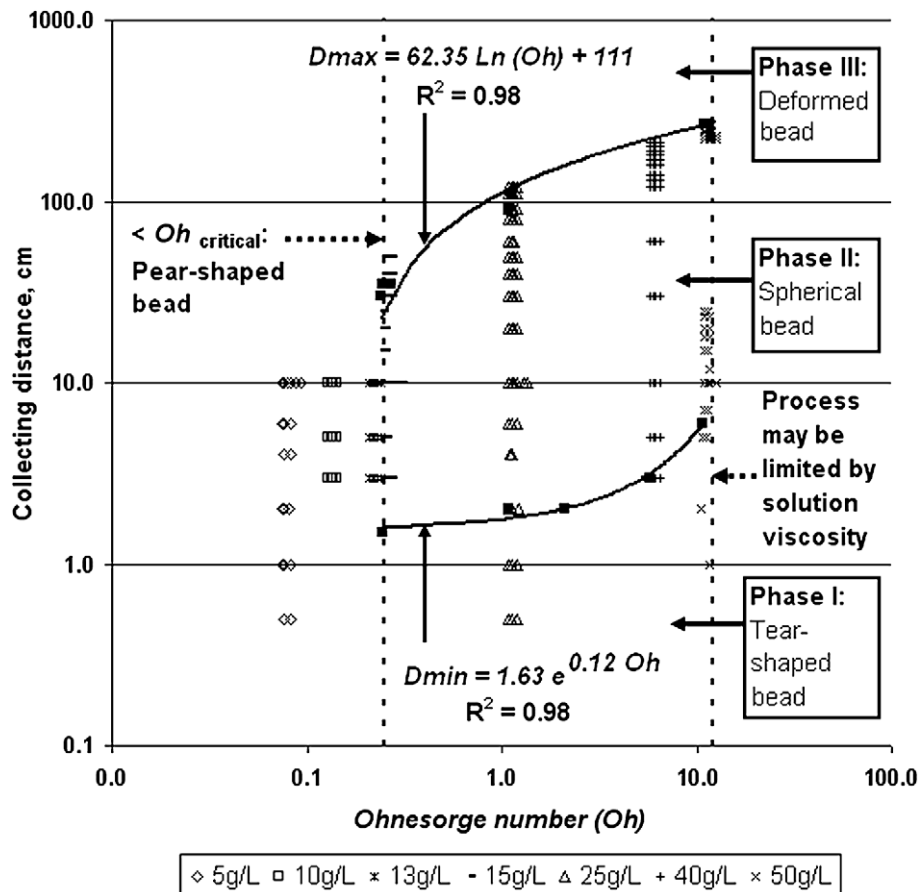


Fig. 4. Correlation between the collecting distance and liquid properties.

The liquid drop mass could be calculated from the volume of the drop, determined through image analysis, and the solution density. The falling drop velocity could be estimated by using a model proposed by Pumphrey and Elmore [30] for rain fall study, as shown in Eq. (7):

$$u = V_T \left[1 - \exp \left(\frac{-2gh}{V_T^2} \right) \right]^{1/2} \quad (7)$$

where u is the velocity of the alginate liquid drop (m/s) at the point of impact, V_T is the terminal velocity (m/s), g is the gravitational acceleration (m/s^2), h is the collecting distance (m) (i.e. the distance between the dripping tip and gelation bath).

The terminal velocity for spherical drop can be estimated from Atlas's model [31], as shown in Eq. (8):

$$V_T = 9.65 - 10.3 \exp(-0.6d_d) \quad (8)$$

where d_d = alginate liquid drop diameter (mm).

As expected, the liquid drop velocities increased with the falling distance and the liquid drop size had little effect on drop velocity. The highest velocity was about 615 cm/s after the liquid drops travelled up to a distance of 270 cm (see Fig. 5). On the other hand, the terminal velocities were about 750–900 cm/s depending on the liquid drop size (i.e. 2.4–4.1 mm). Although the critical momentum could be of interest, it was not determined because the value varied depending on the liquid properties. Alternatively, dimensionless number groups, the Ohnesorge number (Oh) and Reynolds number (Re) at the point of impact, were used to develop the inter-relationships between the process variables involved.

The Ohnesorge number (Oh) measures the importance of the viscous force to surface tension force of the alginate liquid drop as described by Eq. (1). On the other hand, the Reynolds number (Re) measures the importance of the inertia force to viscous force of falling liquid drops and it can be described by Eq. (9):

$$Re = ud_d/1000\nu \quad (9)$$

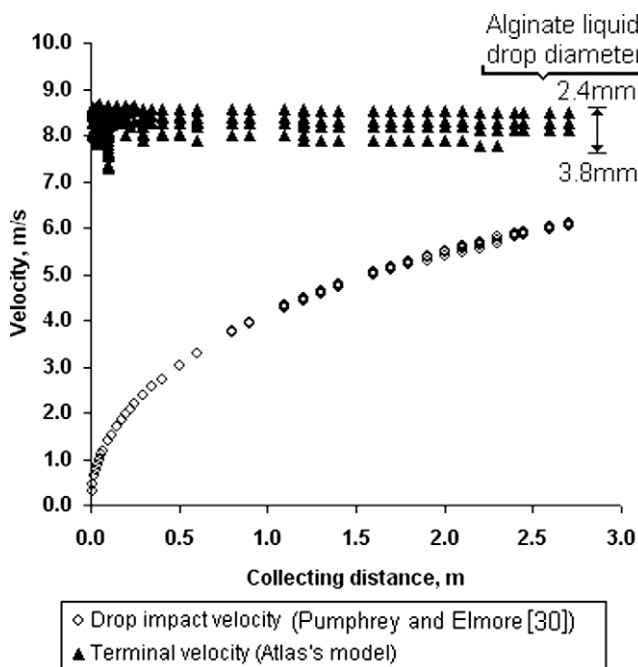


Fig. 5. The impact velocity and terminal velocity of alginate liquid drop at varying distance.

where u is the velocity of the alginate liquid drop (m/s) at the point of impact, d_d is the diameter of the of the alginate liquid drop (mm) and ν is the kinematic viscosity of the alginate solution (mm^2/s).

Fig. 6 shows the shape diagram of the $Oh-Re$ plot that reveals the operating region within which spherical ca-alginate beads could be formed under the experimental conditions. The lower and upper boundaries of the area are dependent on the liquid properties and they are independent of the Reynolds number. The boundaries are given by the critical Ohnesorge number, $Oh=0.24$ and $Oh=11-13$, as shown in Fig. 6. On the other hand, the boundary at the left side of the area is determined by the degree of impact required to transform the less spherical liquid drop to spherical beads. It could be used to describe the transition point between phase I and phase II or the minimum collecting distance to form spherical beads. For the points situated (to the left) outside this boundary, tailed-beads were normally formed due to the partial retainment of the tear-shape liquid drop at a very short collecting distance.

The right boundary of the area varies with the physical properties of the liquid drop and it is given by the equation $Oh = 44Re^{-1.35}$. It reveals the influence of the process variables on the transition points between phase II and phase III. The position of the boundary is reasonable because it suggests that the shape deformation occurs before drop disintegration could take place in a liquid-liquid impact. A drop disintegration equation in a liquid-liquid impact was proposed by Fujimatsu et al. [28] and it is shown with a line in Fig. 6. From the shape deformation equation, the maximum collecting distance allowable for a specific alginate concentration and drop size to form spherical bead could be determined through back-substitution, if required.

The plot of the Ohnesorge number (Oh) and the Reynolds number (Re) could be used as a master shape diagram to describe the inter-relationships between process variables and the overall limits of the process to produce spherical ca-alginate beads. In theory, the application of this diagram can be extended to other extrusion systems as long as the bead formation process involves liquid-liquid impaction. This can be done since the liquid properties, liquid drop diameter and velocity can be measured or estimated for each

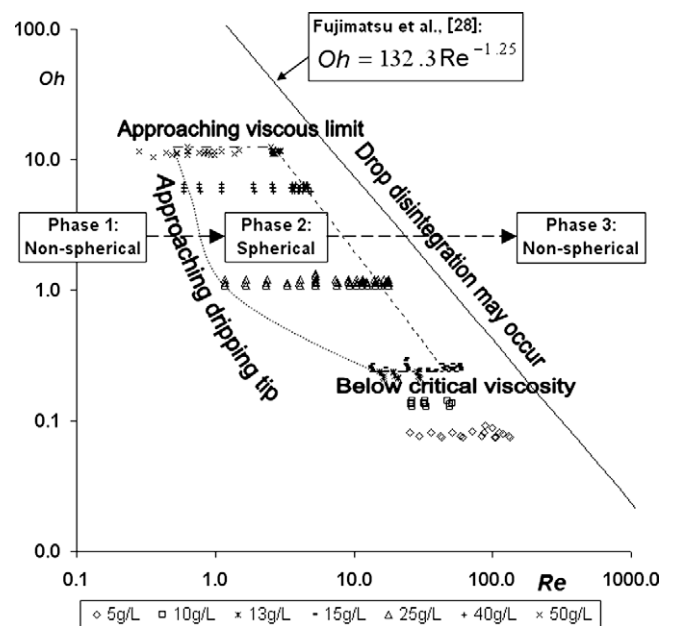


Fig. 6. Shape diagram of ca-alginate beads produced by the extrusion-dripping method. The area within the dotted lines is the proposed operating region for forming spherical particles (Sphericity factor <0.05).

system. In addition, the diagram may also be used to evaluate productivity and process limitations of the chosen system. A free software is currently under development to aid users in the calculation of the dimensionless numbers in the shape diagram. However, the use of this diagram is only limited to the liquid conditions (i.e. alginate and gelling solutions) used in this study. Future work will focus on the effect of the liquid type (e.g. semi-aqueous liquids), surface effects of alginate solutions and gelling bath conditions on the shape diagram.

3.3. Size analysis of alginate drops

For size analysis, an overall size correction factor (K) was introduced to modify the size predicted from Tate's law. The factor was determined through a two-step approach with the aid of image analysis. The liquid lost factor (k_{LF}) was first determined and followed by the determination of the shrinkage factor (k_{SF}). The overall size correction factor (K) was then calculated and the modified Tate's law as described by Eq. (2) was then verified with experimental data to determine the accuracy and applicability in predicting the size of ca-alginate beads.

Under the experimental conditions of this study, the $r/V^{1/3}$ was found to vary from 0.10 to 0.30, which corresponded to the correction factors between 0.73 to 0.90 (see Fig. 7). Therefore, the liquid lost factor (k_{LF}) was calculated from Eq. (3) and the results are shown in Fig. 8. The factor was found to be independent of the liquid properties but it was dependent on the dripping tip size. Within the experimental conditions of this study, the correlation can be described by a linear equation as shown in Eq. (10):

$$k_{LF} = 0.98 - 0.04d_T \tag{10}$$

The shrinkage factor (k_{SF}) was determined next. The percentage shrinkage of the alginate liquid drops after gelation was calculated and shown in Fig. 9. The results show that the shrinkage was neither influenced by the tip size nor the concentration of the alginate solution except for the liquid drop produced from 5 g/L alginate concentration. In this case, the shrinkage was higher than the other alginate concentrations. On the other hand, it was found that the drop shrinkage was mainly influenced by the composition of the M/G ratio. The average shrinkage was about 12% or $k_{SF} = 0.88$ for

low M/G ratio (i.e. Manugel GHB) and 19% or $k_{SF} = 0.81$ for high M/G ratio (i.e. Manuacol DH).

Some studies speculated that the shrinkage of the ca-alginate particles was attributed to the formation of hydrogel network during cross-linking, which could cause water loss and thus reduced the volume of the particles [31,32]. This phenomenon has been known as 'syneresis'. In this study, the ca-alginate beads formed from 0.5% alginate concentration was not spherical and this could lead to inaccuracy in determining the bead size. Despite this, it has been reported that the degree of shrinkage was higher for beads produced from lower alginate concentration [33].

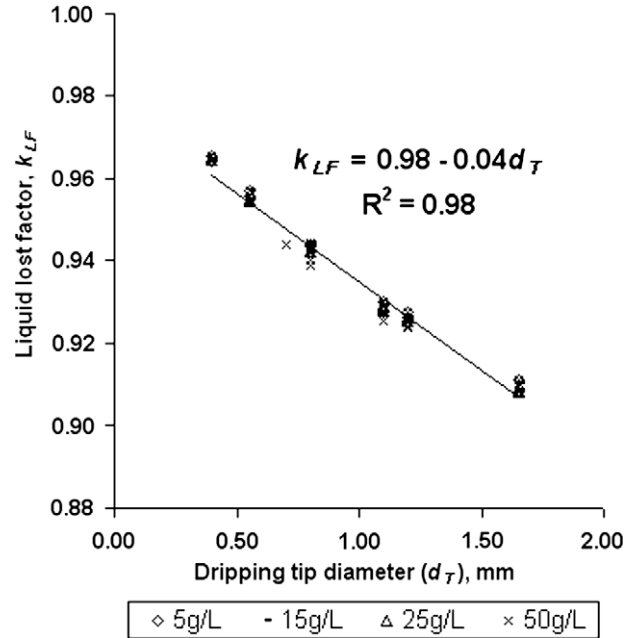


Fig. 8. Effect of dripping tip size on the liquid drop reduction factor, k_{LF} . All points were plotted from Manugel GHB and Manuacol DH.

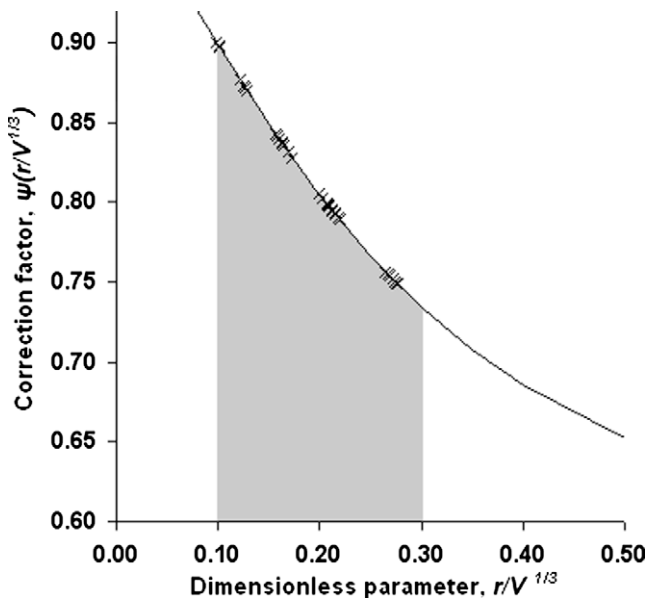


Fig. 7. Determination of HB correction factors ($\Psi(r/V^{1/3})$) from dimensionless tip radius, $r/V^{1/3}$.

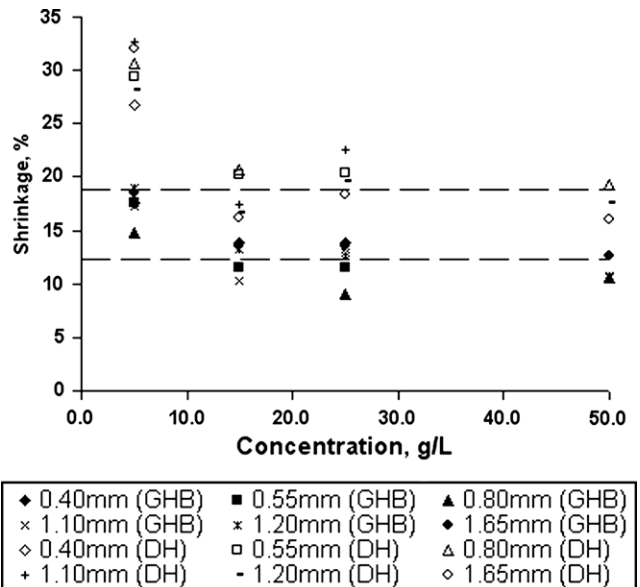


Fig. 9. The shrinkage percentage of alginate liquid drop upon gelation. The details of alginate type and dripping tip diameter are shown in the legend. The collecting distance was set at 10 cm.

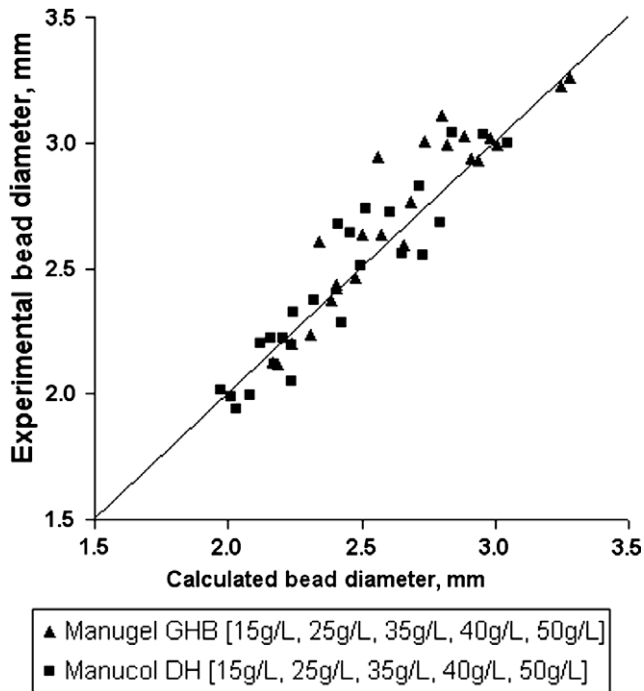


Fig. 10. Validation of the size prediction model. The collecting distance was set at 10 cm. The calculated data: Modified Tate's law equation (Eq. (11)). The average absolute deviation (AAD) is <5%.

Many reports have concluded that the M/G ratio of alginate has major influence on the degree of shrinkage as it affects the gelation mechanism (i.e. 'egg-box' formation) [34–38]. Alginate of lower M/G ratio forms more rigid and porous gel if compared to that of the higher M/G ratio [34,37]. Therefore, lower M/G alginate was found to cause less shrinkage [37–40], which is also in good agreement with this work. Moreover, it has been shown that the degree of shrinkage could vary from 10% to 50% [12,13,31,41,42]. Other possible causes for the variation could be the alginate source, the type and concentration of cross-linking agent, the presence of chelating agent or impurity, as well as the gelling conditions. For example, it was found that the degree of shrinkage increased with the hardening time (data not shown).

Since the liquid lost factor (k_{LF}) and the shrinkage factor (k_{SF}) could be determined, the modified Tate's law could be described in Eq. (11):

$$d_p = k_S(0.98 - 0.04d_T)(0.006d_T\gamma/\rho g)^{1/3} \quad (11)$$

where $k_S = 0.88$ for low M/G ratio (i.e. Manugel GHB) and $k_S = 0.81$ for high M/G ratio (i.e. Manucol DH).

The size prediction model was then verified with experimental data in order to determine its accuracy and applicability in predicting the size of ca-alginate beads as shown in Fig. 10. The results show that the size prediction models are in good agreement with the experimental data, with an average absolute deviation (AAD) of less than 5%. Furthermore, the overall size correction factor (K) was found to be in the range of 0.73–0.85. This gives a good justification to the size reduction constant of 0.85 proposed by Poncelet and Neufeld [43] and Muralidhar et al. [44].

Since the dripping tip diameter used for encapsulation application is normally less than 1 mm, the correlation for k_{LF} (refer to Eq. (10)) could be generally used in the calculation of the overall size correction factor (K). The main limitation of the prediction model is the shrinkage factor (k_{SF}). It could not be an intrinsic part of the model if the materials and gelation conditions were considerably different from this study. In some cases, swelling could occur. For

example, nylon-based particle was found to swell by a factor of 1.3 [13]. Therefore, the k_{SF} could be referred to as the shrinkage or swelling factor and it has to be empirically determined if necessary.

4. Summary

The prediction models for the shape and size of ca-alginate beads produced through the extrusion method were developed in this work. They could be used for process optimization and to evaluate process limitations. The main results of this study are summarized as follows:

- (1) Sphericity factor was found to be an efficient dimensionless shape indicator to study the shape of the alginate drops. The shape of the alginate liquid drops during falling and the ca-alginate beads formed could be distinguished into four basic types: tear-shaped, egg-shaped, pear-shaped and spherical.
- (2) Spherical bead could only be formed when $Oh > 0.24$. Furthermore, the shape transition of ca-alginate beads could be distinguished into three phases along the collecting distance. The transition points of the distance between the phases were mainly dependent on the liquid properties, which can be described by the equations for the minimum and maximum collecting distances.
- (3) A shape diagram which is a plot of the Reynolds number (Re) and the Ohnesorge number (Oh) of liquid drops at the point of liquid–liquid impact, could be used to describe the inter-relationships between all process variables and the bead shape. It reveals a clear operating region and the process limits within which spherical ca-alginate beads could be formed.
- (4) An overall size correction factor (K) could be used to correct the Tate's law in predicting the size of the ca-alginate beads by taking into account the liquid lost factor (k_{LF}) and the shrinkage factor (k_{SF}). The liquid lost factor (k_{LF}) was independent of the liquid properties but was dependent on the tip size. It could be described by a linear equation within the experimental limits. The shrinkage factor (k_{SF}) was found to be affected by the M/G ratio of alginate. The overall size correction factor (K) varied from 0.73 to 0.85 under the experimental conditions and the size prediction model was found to correlate well with the experimental data with an average absolute deviation of less than 5%.

Acknowledgments

The authors would like to thank the Ministry of Science, Technology and Innovation (MOSTI), Malaysia for giving the financial support in this study. The authors also thank colleagues and collaborators who have contributed to the development of this work.

Appendix A

Nomenclature

h	collection distance, cm
ρ	density, kg/m^3
d_d	diameter of alginate liquid drop, mm
d_p	diameter of ca-alginate bead, mm
d_T	outer diameter of tip, mm
g	gravitational force, 9.81 m/s^2
$\Psi(r/V^{1/3})$	HB correction factor in function of $(r/V^{1/3})$
Oh	Ohnesorge number, $Oh = \eta/(\rho d_d \gamma)^{1/2}$
Re	Reynolds number, $Re = (d_d \rho u_{tip})/\eta$

k_{LF}	liquid lost factor
K	overall size correction factor
k_{SF}	shrinkage factor
γ	surface tension, mN/m
η	viscosity, mPa s

References

- [1] K.I. Draget, O. Smidsrod, G. Skjak-Braek, in: A. Steinbuchel, E.J. Vandamme, S. De Baets (Eds.), *Biopolymers 6. Biology Chemistry Biotechnology Application Polysaccharides II Polysaccharides from Eukaryotes*, Wiley-VCH, Verlag GmbH, Weinheim, pp. 215–243.
- [2] G. Fundueanu, C. Nastruzzi, A. Carpov, J. Desbrieres, M. Rinaudo, *Biomaterials* 20 (1999) 1427.
- [3] A. Shilpa, S.S. Agrawal, A.R. Ray, *J. Macromol. Sci. C Polym. Rev.* 43 (2003) 187.
- [4] C. Zohar-Perez, I. Chet, A. Nussinovitch, *Food Hydrocolloids* 18 (2004) 249.
- [5] K.R. Jegannathan, S. Abang, D. Poncelet, E.S. Chan, P. Ravindra, *Crit. Rev. Biotechnol.* 28 (2008) 253.
- [6] K.R. Jegannathan, E.S. Chan, P. Ravindra, *J. Mol. Catal. B: Enzym.* 58 (2009) 78.
- [7] E.S. Chan, Z. Zhang, *Food Bioprod. Process.* 80 (2002) 78.
- [8] E.S. Chan, Z. Zhang, *Process. Biochem.* 40 (2005) 3346.
- [9] O. Smidsrod, G. Skjak-Braek, *TIBTECH* 8 (1990) 71.
- [10] H.A. Al-Hajry, S.A. Al-Maskry, L.A. Al-Kharousi, O. El-Mardi, W.H. Shayya, M.F.A. Goosen, *Biotechnol. Prog.* 15 (1999) 768.
- [11] C. Ouwerx, N. Velings, M.M. Mestdagh, M.A.V. Axelos, *Polym. Gels Netw.* 6 (1998) 393.
- [12] S.B. Seifert, J.A. Philips, *Biotechnol. Prog.* 13 (1997) 562.
- [13] C. Dulieu, D. Poncelet, R.J. Neufeld, in: W.M. Kuhtrierer, R.P. Lanza, W.L. Chick (Eds.), *Cell Encapsulation Technology and Therapeutics*, Birkhauser, Boston, 1999, pp. 3–17.
- [14] D. Poncelet, V.G. Babak, R.J. Neufeld, M.F.A. Goosen, B. Burgarski, *Adv. Colloid Interface Sci.* 79 (1999) 213.
- [15] C. Heizen, A. Berger, I. Marison, in: V. Nedovic, R. Willaert (Eds.), *Kluwer Academic Publishers.*, London, UK, 2004, p. 262.
- [16] B.B. Lee, P. Ravindra, E.S. Chan, *Colloids Surf. A: Physicochem. Eng. Aspects* (2009) 112.
- [17] B.B. Lee, P. Ravindra, E.S. Chan, *Chem. Eng. Commun.* 195 (2008) 889.
- [18] W.D. Harkins, F.E. Brown, *J. Am. Chem. Soc.* 41 (1919) 499.
- [19] P. Del Gaudio, P. Colombo, G. Colombo, P. Russo, F. Sonvico, *Int. J. Pharm.* 302 (2005) 1.
- [20] H. Watanabe, T. Matsuyama, H. Yamamoto, *J. Electrostat.* 57 (2003) 183.
- [21] D.F. Day, in: D.L. Kaplan (Ed.), *Biopolymers from Renewable Resources*, Springer-Verlag Berlin Heidelberg, Berlin, Germany, 1998, pp. 119–143 (Chapter 5).
- [22] E.P. Herrero, E.M.M. Del Valle, M.A. Galan, *Chem. Eng. J.* 117 (2006) 137.
- [23] W. Sabra, W. Deckwer, in: D. Severian (Ed.), *Polysaccharides. Structural Diversity and Functional Versatility*, second ed., Markel Dekkar, New York, 1998, pp. 515–531 (Chapter 21).
- [24] J.F. Steffe, *Rheological Methods in Food Processing Engineering*, second ed., Freeman Press, East Lansing, USA, 1996, pp. 1–91.
- [25] V.G. Babak, E.A. Skotnikova, L.G. Lukina, S. Pelletier, P. Hubert, E. Dellacherie, *J. Colloid Interface Sci.* 225 (2000) 505.
- [26] V. Hershko, A. Nussinovitch, *Biotechnol. Prog.* 14 (1998) 756.
- [27] J.R. Saylor, N.K. Grizzard, *Exp. Fluids* 36 (2004) 783.
- [28] T. Fujimatsu, H. Fujita, M. Hirota, O. Okada, *J. Colloid Interface Sci.* 264 (2003) 212.
- [29] K.Y. Lee, T.R. Heo, *App. Environ. Microbiol.* 66 (2000).
- [30] H.C. Pumphrey, P.A. Elmore, *J. Fluid Mech.* 220 (1990) 539.
- [31] J. Chrastil, *J. Agric. Food Chem.* 39 (1991) 874.
- [32] N.M. Velings, M.M. Mestdagh, *Polym. Gels Netw.* 3 (1995) 311.
- [33] H. Brandenberger, F. Widmer, *J. Biotechnol.* 63 (1998) 73.
- [34] G. Klock, A. Pfeffermann, C. Ryser, P. Grohn, B. Kuttler, H. Hahn, U. Zimmermann, *Biomaterials* 18 (1997) 707.
- [35] W.F. Kendall Jr., M.D. Darrabie, H.M. El-Shewy, E.C. Opara, *J. Microencapsul.* 21 (2004) 821.
- [36] N.E. Simpson, S.C. Grant, S.J. Blackband, I. Constantinidis, *Biomaterials* 24 (2003) 4941.
- [37] N.E. Simpson, C.L. Stabler, C.P. Simpson, A. Sambanis, I. Constantinidis, *Biomaterials* 25 (2004) 2603.
- [38] B. Thu, O. Smidsrod, G. Skjak-Braek, in: R.H. Wijffels, B.M. Buitelaar, C. Bucke, J. Tramper (Eds.), *Elsevier Science, B.V.*, Amsterdam, 1996.
- [39] W.R. Gombotz, S.F. Wee, *Adv. Drug Deliv. Rev.* 31 (1998) 267.
- [40] S. Takka, F. Acarturk, *J. Microencapsul.* 16 (1999) 275.
- [41] W. Van Beinum, J.C.L. Meeussen, W.H. Van Riemsdijk, *Environ. Sci. Technol.* 34 (2000) 4902.
- [42] T.I. Klokk, J.E. Melvik, *J. Microencapsul.* 19 (2002) 415.
- [43] D. Poncelet, R.J. Neufeld, in: R.H. Wijffels, R.M. Buitelaar, C. Bucke, J. Tramper (Eds.), *Immobilized Cells: Basics and Applications*, Elsevier Science B.V., Amsterdam, 1996, pp. 47–53.
- [44] R.V. Muralidhar, G. Jayachandran, P. Singh, *Curr. Sci.* 81 (2001) 263.